Introduction to LIGO and an Experiment Regarding the Quality Factor of Crystalline Silicon

A Senior Project

Presented by Edward Taylor

With Mentorship from Dr. Thomas Gutierrez

To the Faculty of the Cal Poly, San Luis Obispo Physics Department

06/16/2014

Third generation LIGO detectors will be limited by thermal noise at a low frequency band where gravitational wave signals are expected to exist. A large contribution to thermal noise is caused by internal friction of the mirror and suspension elements. In order to meet the quantum mechanical sensitivity limits of the detector, it will be necessary to further push down the contribution of thermal noise. Future detectors will require new materials with extremely high mechanical quality. Silicon at cryogenic temperatures shows the promise to provide the required mechanical quality due to its vanishing expansion coefficient at 120 K. The fluctuation dissipation theorem links thermal noise to mechanical dissipation which, in turn, motivates us to study the quality factor of silicon cantilevers. An experiment is designed to measure the mechanical quality of silicon flexures at cryogenic temperatures. Utilizing a ring-down method in vacuum, we determine the quality factor of a silicon cantilever at room temperatures. Q-factors of up to $2.84 \cdot 10^5$ were measured. Further experiments should be performed at cryogenic temperatures with etched samples to determine how the quality factor is impacted. In addition, an introduction to LIGO and the respective sources of noise is presented.

Figure 1: A picture of the LIGO Livingston site with the two perpendicular arms that extend for 4 kilometers.

1. Introduction

The idea of gravitational waves comes from the work of Albert Einstein in the early 20th century. During this time, Einstein revamped Newtonian gravitational theory by showing that local mass-energy is equivalent to local space-time curvature. This was quantified in the Einstein field equations which are a set of non-linear partial differential equations (Equation 1) [1].

$$R_{\mu\nu} - \frac{1}{2} g_{\mu\nu} R + g_{\mu\nu}\Lambda = \frac{8\pi G}{c^4} T_{\mu\nu} \qquad (1)$$

Here $R_{\mu\nu}$ is the Ricci curvature tensor, $g_{\mu\nu}$ is the metric tensor, R is the scalar curvature, Λ is the cosmological constant, G is Newton's gravitational constant, c is the speed of light in vacuum, and $T_{\mu\nu}$ is the stress-energy tensor. In addition to implying a number of phenomena, wave solutions exist for these equations.

Gravitational waves have never been directly observed before but there is little doubt that they exist. Gravitational waves are implied by Einstein's theory of relativity, which has accumulated numerous experimental confirmations since its postulation. Newtonian gravity does not provide for gravitational radiation and thus, changes in the gravitational field must be transmitted at infinite speed. This violates the already confirmed special theory of relativity, which states that information cannot be transmitted faster than the speed of light. Since special relativity has already been confirmed on numerous occasions, it is accepted that gravitational waves must propagate at the speed of light or less.

The geometry of space-time can be expressed by the metric tensor $g_{\alpha\beta}$ which connects the space-time coordinate dx^{α} (Where $\alpha = 0,1,2,3$) to the spacetime interval ds [1]:

$$ds^2 = g_{\alpha\beta} dx^{\alpha} dx^{\beta} \tag{2}$$

The gravitational waves far from any substantial source of gravity will be very weak. We can then approximate the background metric as the flat Minkowski metric and, subsequently, the gravitational wave field as the sum of this flat metric and a small perturbation [1]:

$$g_{\alpha\beta} = \eta_{\alpha\beta} + h_{\alpha\beta} \tag{3}$$

To obtain an explicit solution of the metric perturbation h it is necessary to make a gauge choice. The most useful gauge with regards to this context is the transverse traceless gauge. In this gauge, and in the weak field limit discussed above, the Einstein equations become a system of linear equations, specifically a system of wave equations [1]:

$$\left(\nabla^2 - \frac{1}{c^2}\frac{\partial^2}{\partial t^2}\right) h_{\alpha\beta} = 0 \tag{4}$$

This equation tells us that gravitational waves travel at the speed of light and that the gravitational wave tensor h can be considered to be the gravitational wave field. The wave field is transverse and traceless and for waves traveling in the z direction, it can be expressed as follows [1]:

$$h_{\alpha\beta} = \begin{pmatrix} 0 & 0 & 0 & 0 \\ 0 & h_{xx} & h_{xy} & 0 \\ 0 & h_{yx} & h_{yy} & 0 \\ 0 & 0 & 0 & 0 \end{pmatrix} \tag{5}$$

Since the Riemann tensor is symmetric, h also satisfies:

$$h_{yx} = h_{xy} \tag{6}$$

This symmetry implies that there two possible polarization states which are denoted $h_\times$ and h_+ and can be expressed as follows [1]:

$$h_+ = Re[A_+ e^{-i\omega\left(t-\frac{z}{c}\right)}] \tag{7}$$

$$h_\times = Re[A_\times e^{-i\omega\left(t-\frac{z}{c}\right)}] \tag{8}$$

These solutions resolve the problem with instantaneous action-at-a-distance of Newtonian gravitation theory. More importantly, they imply that the gravitational field moves with the speed of light in turn bringing news of space-time curvature at a finite speed [1].

Experiments aiming to detect gravitational waves produced by large astronomical events have been underway for the past 40 years but only now have sensitivities reached a level where detection is a real possibility within the next few years. LIGO, a large scale physics experiment consisting of the most sensitive gravitational wave detectors in the world, is expected to detect a gravitational wave that may originate from coalescing neutron stars and black holes, spinning neutron stars, and supernovas [2]. Each detector is essentially a Michelson interferometer which consists of mirror test masses suspended as pendula whose displacements are detected by measuring subsequent phases of lasers reflected off of the masses (Figure 2).

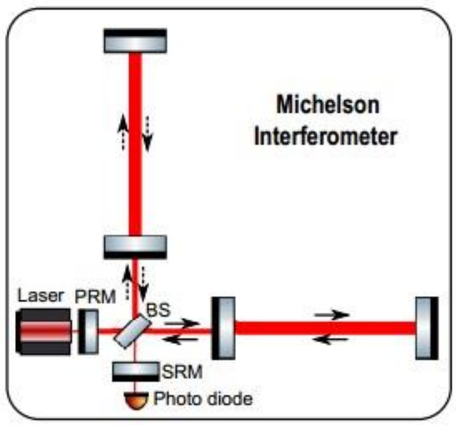

Figure 2: A Schematic of the Michelson interferometer consisting of Fabry-Perot arm cavities.

These displacements occur when a gravitational wave passes and distorts space-time through the detector. The strain that would be detected by the interferometer is limited by a number of noise sources including seismic noise, shot noise, radiation pressure, and thermal noise. Figure 3 displays the projected noise of all sources for advanced LIGO. Research has already begun on how to reduce noise for 3rd generation LIGO interferometers. For instance, radiation pressure will be addressed using squeezed light and filter cavities [3]. Once this radiation pressure is reduced, thermal suspension noise will be a significant source of noise at low frequencies. The thermal noise associated with the mirror masses' suspensions is one of the most significant noise sources in a frequency band centered on 100 Hz [4]. This prompts us to investigate the effects of thermal noise on the suspension. But first, let us take a look at the various sources of noise inherent in the detector.

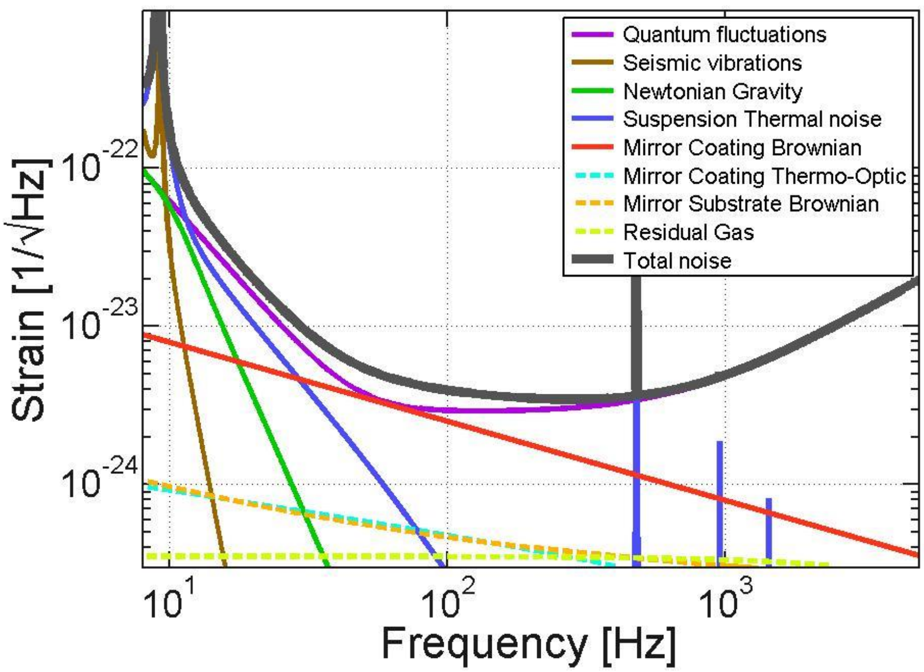

Figure 3: The projected effect of various noise sources for the Advanced LIGO detector

The above figure shows the effect of the different noise sources for the upgraded LIGO detector. Shot noise falls under the category of quantum noise and its main limitation to the sensitivity of the LIGO interferometers comes at about frequencies above 100 Hz [4]. To understand shot noise, we must first consider Poisson statistics. Poisson statistics come into play in systems where there is some event whose probability of occurring in a fixed time interval is constant. Photons emitted from a laser beam obey the Poisson distribution:

$$p(n) = \frac{\mu^{-n} e^{-\mu}}{n!} \quad (9)$$

Where μ is the expected number of photons, n is the number of photons and $p(n)$ is the probability of observing that amount of photons. The Poisson distribution is unique by the fact that the standard deviation is equal to the square root of the average. So now, we may go about thinking of the laser beam as particles (photons). Or, we may go about thinking of the beam as waves. It turns out that the laser beam is both wave-like and particle-like but we are not surprised by this since wave-particle duality applies. When the beam is in a wave-like state there is an uncertainty associated with the phase. When the beam is in more of a particle-like state, there is an uncertainty associated with the number of particles. The product of these two uncertainties must be greater than or equal to 1 (Heisenberg uncertainty). Therefore, the uncertainty of the phase is directly related to the uncertainty in the number of particles. The uncertainty in the phase of a laser beam due to quantization of light is called shot noise [4].

Seismic noise is the result of ground motion coupling to the motion of the mirrors. It can be suppressed in multiple ways such as suspending the mirrors as pendula or by sensing ground motion and actively feeding this back into cancellation controls [4].

Mirror coating noise is associated with thermal noise in the coatings. Thermal noise is described in the next section.

1.1 Thermal Noise

The first insight into thermal noise began in 1828 when Robert Brown observed a ceaseless jiggling of pollen molecules suspended in water [4]. Later, Einstein showed that the fluctuations of the pollen particles arose from the impacts of water molecules on the grain. Specifically, he theorized that the mean-square displacement of a particle is

$$\overline{x_{Therm}^2} = k_B T \frac{1}{3\pi a\eta} \tag{10}$$

Where τ is the duration of observation, a is the radius of a spherical grain, and η is the viscosity of the fluid [4]. In itself, the equation represents a link between the random fluctuations of the particle to the mechanism for dissipation i.e. the viscosity of the water. The example of Brownian noise is a special case of the fluctuation-dissipation theorem which relates the dissipation of a dynamical system with its equilibrium thermal fluctuations [2]. Specifically, the theorem connects the linear relaxation of a system in a non-equilibrium state to its statistical fluctuations in equilibrium [5]. The theorem was further quantified in 1928 when Johnson and Nyquist showed that the mean-square voltage of a resistor depends on the resistance:

$$\langle V^2 \rangle = 4Rk_B T\Delta\nu \tag{11}$$

Where $\Delta\nu$ is the bandwidth over which the voltage is measured, V^2 (the voltage squared) is a sort of a generalized fluctuating force and R (the resistance) represents dissipation. This means that any sort of dissipation guarantees fluctuating forces when the system is at rest which, in the case of LIGO's mirrors and mirror suspensions, masks the signal that one attempts to observe. However, it also implies that one does not need to make a detailed microscopic model of any dissipation phenomenon in order to predict the fluctuation associated with it [4].

The theorem shows us that the way to reduce the level of thermal noise is to reduce the amount of dissipation. However, this would be against our intuition since the equipartition theorem guarantees $\frac{1}{2}k_B T$ of energy for the mean value of each quadratic degree of freedom in a system. Thus, one would think that the only way to reduce fluctuation is through a reduction of temperature. But, the equipartition theorem speaks of the *mean* value of quadratic terms thus implying an integral over all values of the particular degree of freedom. This means that the integral of the thermal noise power spectrum over all frequencies is independent of dissipation. For the case of a damped forced oscillator, the fluctuation-dissipation theorem gives the relationship between loss and displacement noise at a *certain frequency*. At the resonant frequency, displacement noise is inversely proportional to mechanical loss and off resonance, it is directly proportional. This means that we can rearrange fluctuation energy if we decrease the mechanical loss and thus funnel that noise into the resonant frequencies. This, in turn, prompts us to examine low loss materials and investigate other parameters that will minimize thermal noise in the suspension system of the 3rd generation LIGO project. Currently, advanced LIGO operates on fused silica as the mirror substrate and suspension fiber but a demand for an increase in sensitivity of the detector opens new candidates that may be used in 3rd generation detectors. Silicon is a promising candidate for test masses and suspension elements due to its vanishing coefficient of thermal expansion and excellent mechanical and optical properties [6]. Our aim is to investigate the mechanical dissipation of silicon flexures by calculating its quality factor at various temperatures and for a number of frequencies.

1.2 Sources of Thermal Noise

The main sources of thermal noise for crystalline silicon are external, thermoelastic, phonon-phonon, and surface loss. External noise comes from friction at the point of suspension or collisions with residual gas particles. External sources of dissipation, however, are relatively miniscule sources of noise and can be neglected for our purposes. Phonon-phonon noise arises from a modulation of lattice vibrations when an external oscillation is applied with a wavelength much longer than the wavelength of thermal phonons. This redistribution of all phonons generates entropy and is thus a loss mechanism, however, it is only a significant contributor to noise at low temperatures. Thermoelastic loss arises from the fact that when a sample is bent, one side of it is heated and the other is cooled. The local temperature difference causes a heat flux which increases entropy and thus dissipates energy. Surface loss originates from cracks and contaminations in a small surface layer of the silicon, however, it is not fully understood. The expected contribution to mechanical loss of a silicon flexure from thermoelastic and phonon-phonon loss is displayed in figure 4. Our effort was focused around measuring the thermoelastic loss at room temperature.

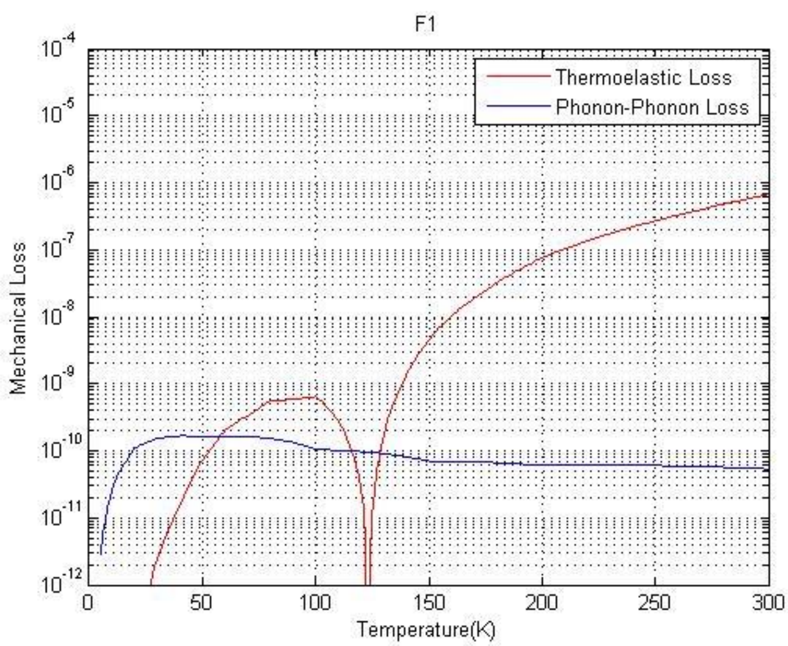

Figure 4: Summary of possible mechanical loss sources of a silicon flexure at 70 Hz

2. Experimental Design

In 2013, I spent a summer at Cal Tech and performed this experiment under the supervision of a post-doctorate physicist. Our primary goal was to measure the quality factor of a thin silicon flexure and, in turn, quantify the amount of thermal noise at different resonant frequencies. The quality factor is a dimensionless parameter that describes how under-damped an oscillator or resonator is. Equivalently, the Q-factor is a resonator's bandwidth relative to its center frequency.

The initial apparatus consisted of a HeNe laser, cryostat (figure 5), stainless steel clamp, aluminum corner reflector, electrostatic driving plate, PEEK insulator, and a thin silicon flexure. The components within the cryostat are displayed in figure 6. In order to measure a mechanical quality factor, the silicon flexure must be excited into oscillatory motion. The electrostatic driving plate (ESD) produces a non-uniform electrodynamic field which, when placed near the silicon flexure, forces the cantilever to oscillate. A signal generator and high-voltage source provided the ESD's power and allowed a manual input of the signal's frequency and amplitude. To minimize vibrational losses, the silicon cantilever was clamped down with stainless steel blocks. To achieve a reasonable amount of heat transfer between the cantilever and cryostat, a thin layer of PEEK was inserted beneath the clamp. The clamp attached to the cantilever via screws which were made of silver in order to prevent cold welding. The signal readout of the oscillation consisted of directing the laser through the side of the cantilever and reflecting it back out onto a split photodiode which could then translate a projected oscillatory shadow into a voltage difference. This signal was amplified, sent to an oscilloscope, and then displayed onto a spectrum analyzer.

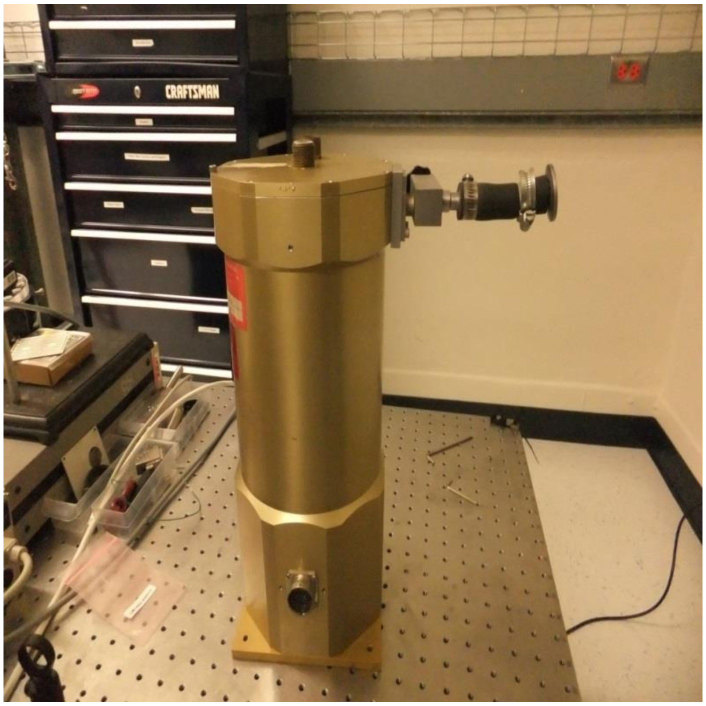

Figure 5: The initial cryostat with no vacuum or electronic attachments

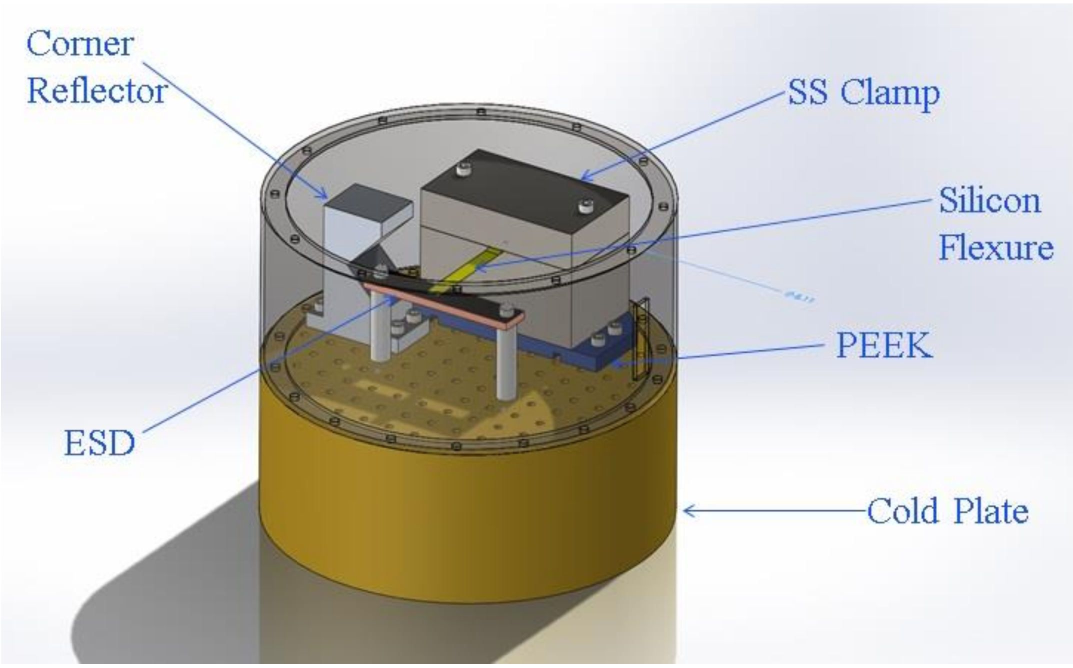

Figure 6: A SolidWorks drawing of the internal components to the cryostat

Due to time constraints, the focus was switched to measuring the Q factor at room temperature. A new vacuum chamber (figure 7) was utilized allowing us to simply transfer the clamp, cantilever and ESD. The chamber had two port windows which allowed us to direct the laser through the vessel and onto the photodiode without the need to reflect back out. The split photodiode itself was constructed by gluing two photodiodes adjacent to each other (figure 8). A ring-down method was employed which consisted of exciting the cantilever to a resonant frequency (a frequency which stimulates a maximum amount of oscillation), turning off the excitation, and observing the expected exponential decay of an under-damped oscillator:

$$x(t) = Ae^{-bt/2m}\cos(\omega t - \phi) \tag{12}$$

The free-decaying amplitude follows an exponential law of the form [7]:

$$a(t) = a_0 \cdot e^{-\frac{t}{\tau}} \tag{13}$$

The characteristic ring-down time τ is used to determine the quality factor [7]:

$$Q = \pi \upsilon_0 \tau \tag{14}$$

Where υ_0 is the temperature dependent resonant frequency. The quality factor is related to the mechanical loss (In this case, thermoelastic) by:

$$Q(\omega) = \frac{1}{\phi(\omega)} \tag{15}$$

In turn, the mechanical loss angle at 6 resonant modes was measured.

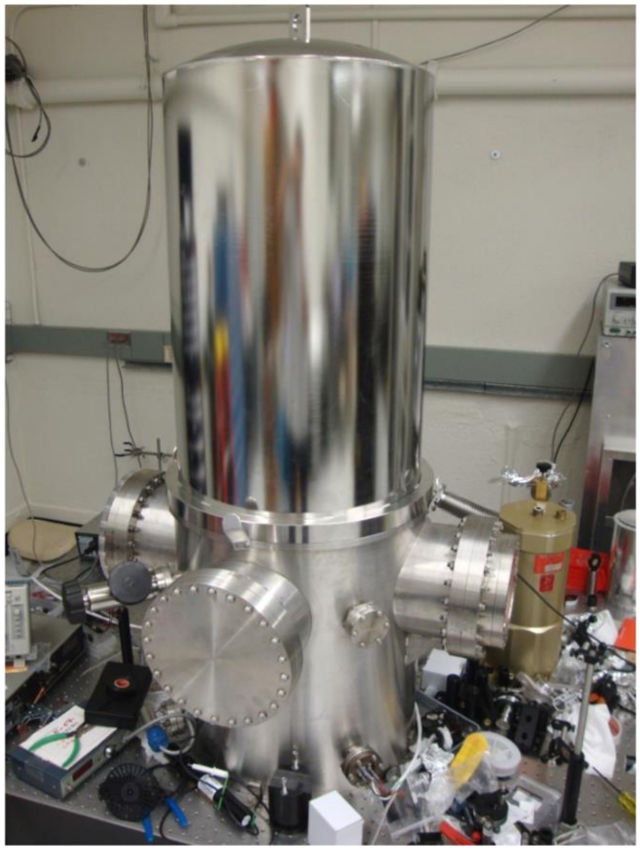

Figure 7: A new vacuum chamber with dual port windows

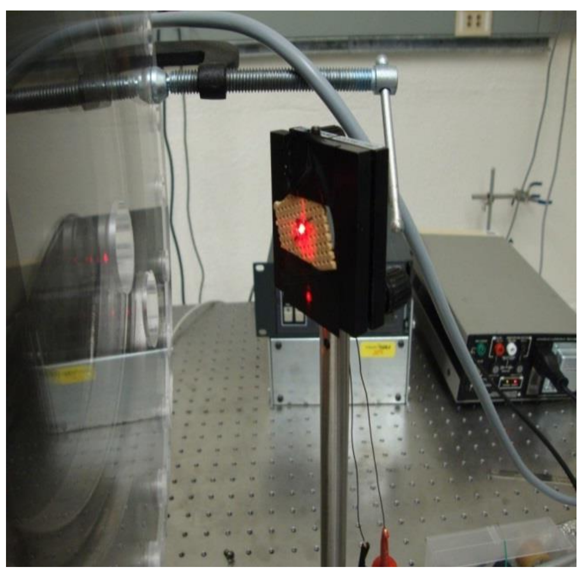

Figure 8: The split photodiode with the laser directed onto it

3. Results

Six eigen-modes of the silicon cantilever were determined using Comsol, a finite element analysis program.

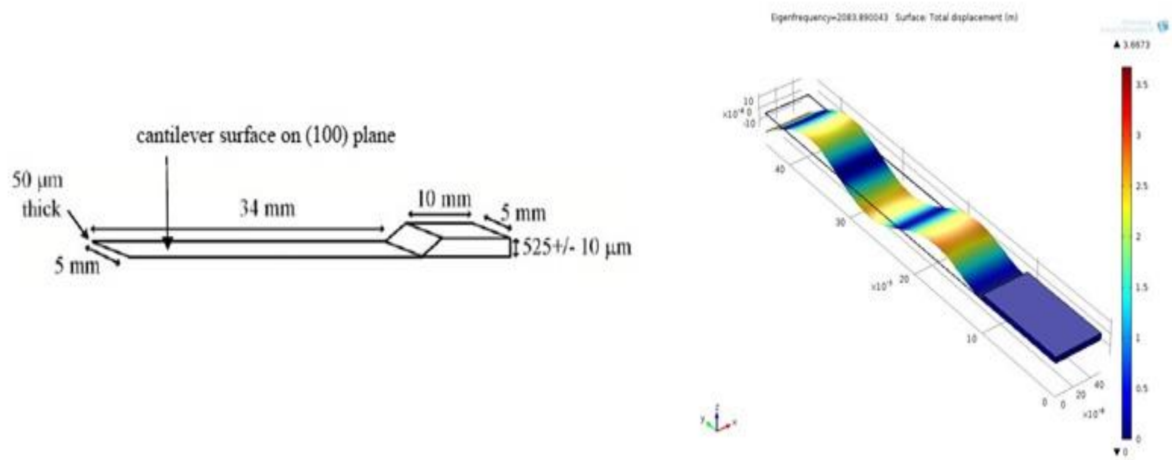

Figure 9: A sketch of the geometry of the silicon cantilever (left). A Comsol model of a bending mode of oscillation (right). The relative displacement is indicated by the color in the legend.

A time series of a decaying oscillation was extracted with a data acquisition system and inputted into Matlab. At consecutive instances of the time series, the sinusoidal data was inputted into the pwelch function in Matlab which produced a power spectral density (PSD) for the resonant mode of interest. The power value of the resonant peak was extracted at each instant and plotted separately. The resonant peaks decayed exponentially with time (since the power is proportional to the amplitude squared of the oscillation), thus, the extracted values were subsequently fitted with equation 13 (Figure 10). The characteristic ring-down time,τ, was inputted into equation 14 to determine the quality factor and mechanical loss. The main contribution to the loss was expected to originate from the thermoelastic loss. For the special case of pure bending modes in crystalline silicon, the equation for the thermoelastic loss is given by:

$$\phi_{TE} = \frac{\alpha^2 Y T}{\rho C_p} \frac{\omega\tau}{1+\omega^2\tau^2} \tag{16}$$

Where α is the thermal expansion coefficient, Y is Young's modulus, and τ is a relaxation time. Note that the internal loss is related to the sample dimension through the relaxation time:

$$\tau = \frac{\rho C_p t^2}{\pi\kappa} \tag{17}$$

Where t is the thickness of the sample.

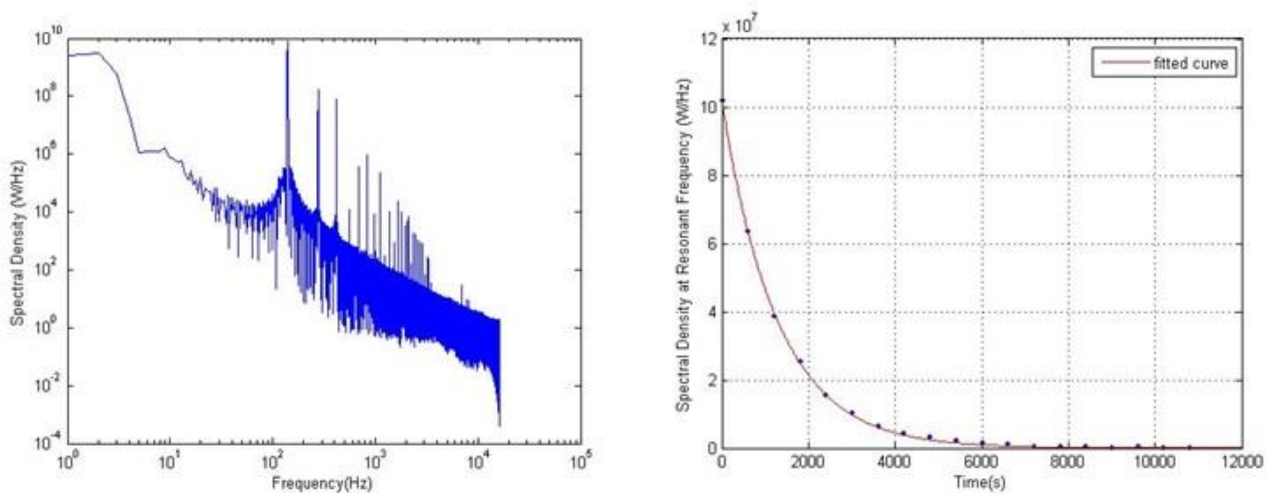

Figure 10: PSD of the first bending mode displaying a peaked intensity at the resonant frequency and peaks at various harmonics (left). Decaying power of the first resonant frequency oscillation fitted to an exponential curve (right).

Figure 11 represents the measured and expected mechanical loss at resonant modes of 70.5 Hz, 536 Hz, 960.4 Hz, 1484.8 Hz, 2910.13 Hz, and 4804 Hz.

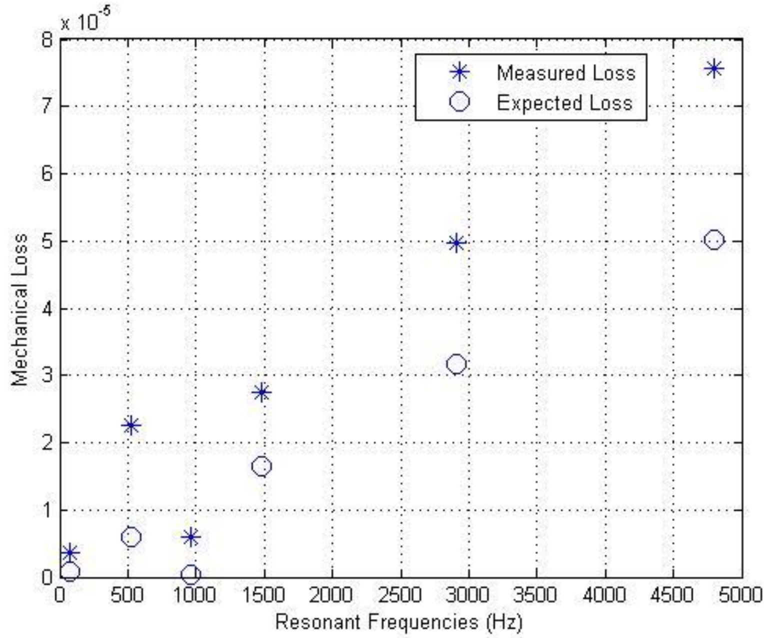

Figure 11: Expected and measured thermoelastic loss plotted for various resonant frequencies 70.5 Hz, 536 Hz, 960.4 Hz, 1484.8 Hz, 2910.13 Hz, and 4804 Hz.

The second mode appears to show excessive loss which may have been due to a misalignment of the laser. The third mode is a torsional mode which is inaccurately modeled by the thermoelastic equation for loss, thus, its expected loss is a rough approximation. This is due to the fact that the heat flux established in a torsional mode is across the width of the cantilever. Nevertheless, the relaxation time is larger and the approximation for the torsional thermoelastic loss is smaller. The first mode shows the lowest mechanical loss with a value of $3.52 \cdot 10^{-6}$ while the highest loss is seen in the highest resonant frequency with a value of $7.56 \cdot 10^{-5}$. Overall, a systematic error is apparent since all of the measured loss values overestimate the expected loss. This may be associated with energy losses to the clamp and the mount upon which it was attached to.

Most likely it originates from surface losses which must be investigated in the future along with how etching techniques may alleviate it.

4. Summary

The mechanical quality factor of a silicon cantilever was measured at room temperature for various resonant frequencies. The measurements confirm that silicon is a high-Q material and is well suited to be used as an optical substrate for future gravitational detectors. Q-factors up to $2.84 \cdot 10^5$ were measured at 300 K. Further work must be done to measure the Q factor at cryogenic temperatures. In addition, it will be necessary to investigate the effect of cantilever dimensions, crystal direction, and etching techniques on the measured Q-factor.

The future of gravitational wave detectors is a bright one, as all the noise sources mentioned above are being addressed by scientists around the world. The noise contribution will continue to be pushed down and it will only be a matter of time before LIGO detects a gravitational wave. This will hopefully spark a new field in physics that will probe the universe through a different lens. Astronomers have always observed the universe through electromagnetic radiation but now, we will be able to see a completely new signature of the world around us.

5. References

[1] Hartle, J. B. Gravity: *An Introduction to Einstein's General Relativity*. San Francisco: Addison-Wesley, 2003. Print.

[2] Callen, Herbert B., and Theodore A. Welton. "Irreversibility and Generalized Noise." *Physical Review* 83.1 (1951): 34-40. Print.

[3] Evans, M., L. Barsotti, J. Harms, P. Kwee, and H. Miao. "Realistic Filter Cavities for Advanced Gravitational Wave Detectors." (n.d.): n. pag. *ArXiv*. Web.

[4] Saulson, Peter R. *Fundamentals of Interferometric Gravitational Wave Detectors*. Singapore: World Scientific, 1994. Print.

[5] Chandler, David (1987). *Introduction to Modern Statistical Mechanics.* Oxford University Press. P. 255. Print.

[6] Nawrodt, Ronny. "Investigation of Mechanical Losses of Thin Silicon Flexures at Low Temperatures." (n.d.): n. pag. *ArXiv*. 15 Mar. 2010. Web.

[7] Abbott, B., R. Abbott, R. Adhikari, A. Ageev, B. Allen, R. Amin, S. B. Anderson, W. G. Anderson, M. Araya, H. Armandula, F. Asiri, P. Aufmuth, C. Aulbert, S. Babak, R. Balasubramanian, S. Ballmer, B. C. Barish, D. Barker, C. Barker-Patton, M. Barnes, B. Barr, M. A. Barton, K. Bayer, R. Beausoleil, K. Belczynski, R. Bennett, S. J. Berukoff, J. Betzwieser, B. Bhawal, I. A. Bilenko, G. Billingsley, E. Black, K. Blackburn, B. Bland-Weaver, B. Bochner, L. Bogue, R. Bork, S. Bose, P. R. Brady, V. B. Braginsky, J. E. Brau, D. A. Brown, S. Brozek, A. Bullington, A. Buonanno, R. Burgess, D. Busby, W. E. Butler, R. L. Byer, L. Cadonati, G. Cagnoli, J. B. Camp, C. A. Cantley, L. Cardenas, K. Carter, M. M. Casey, J. Castiglione, A. Chandler, J. Chapsky, P. Charlton, S. Chatterji, Y. Chen, V. Chickarmane, D. Chin, N. Christensen, D. Churches, C. Colacino, R. Coldwell, M. Coles, D. Cook, T. Corbitt, D. Coyne, J. D. E. Creighton, T. D. Creighton, D. R. M. Crooks, P. Csatorday, B. J. Cusack, C. Cutler, E. D’Ambrosio, K. Danzmann, R. Davies, E. Daw, D. DeBra, T. Delker, R. DeSalvo, S. Dhurandhar, M. Díaz, H. Ding, R. W. P. Drever, R. J. Dupuis, C. Ebeling, J. Edlund, P. Ehrens, E. J. Elliffe, T. Etzel, M. Evans, T. Evans, C. Fallnich, D. Farnham, M. M. Fejer, M. Fine, L. S. Finn, É. Flanagan, A. Freise, R. Frey, P. Fritschel, V. Frolov, M. Fyffe, K. S. Ganezer, J. A. Giaime, A. Gillespie, K. Goda, G. González, S. Goßler, P. Grandclément, A. Grant, C. Gray, A. M. Gretarsson, D. Grimmett, H. Grote, S. Grunewald, M. Guenther, E. Gustafson, R. Gustafson, W. O. Hamilton, M. Hammond, J. Hanson, C. Hardham, G. Harry, A. Hartunian, J. Heefner, Y. Hefetz, G. Heinzel, I. S. Heng, M. Hennessy, N. Hepler, A. Heptonstall, M. Heurs, M. Hewitson, N. Hindman, P. Hoang, J. Hough, M. Hrynevych, W. Hua, R. Ingley, M. Ito, Y. Itoh, A. Ivanov, O. Jennrich, W. W. Johnson, W. Johnston, L. Jones, D. Jungwirth, V. Kalogera, E. Katsavounidis, K. Kawabe, S. Kawamura, W. Kells, J. Kern, A. Khan, S. Killbourn, C. J.

Killow, C. Kim, C. King, P. King, S. Klimenko, P. Kloevekorn, S. Koranda, K. Kötter, J. Kovalik, D. Kozak, B. Krishnan, M. Landry, J. Langdale, B. Lantz, R. Lawrence, A. Lazzarini, M. Lei, V. Leonhardt, I. Leonor, K. Libbrecht, P. Lindquist, S. Liu, J. Logan, M. Lormand, M. Lubinski, H. Lück, T. T. Lyons, B. Machenschalk, M. MacInnis, and M. Mageswaran. "Analysis of LIGO Data for Gravitational Waves from Binary Neutron Stars." *Physical Review* 69 (2004): n. pag. Print.

[8] Nawrodt, R., A. Zimmer, T. Koettig, C. Schwarz, D. Heinert, M. Hudl, R. Neubert, M. Thürk, S. Nietzsche, W. Vodel, P. Seidel, and A. Tünnermann. "High Mechanical Q-factor Measurements on Silicon Bulk Samples." *Journal of Physics: Conference Series* 122 (2008): 012008. Print.

Acknowledgments

The author would like to thank Nicolas Smith-Lefebvre, the mentor of the experiment. Without his help and guidance, none of this would have been possible. Much gratitude also goes to Alastair Heptonstall and Matt Abernathy who provided much needed advice and input for the setup of the apparatus. A big thank you must go to Cal Tech and the scientists of West Bridge who are spearheading the effort to detect gravitational waves. Last but not least, I must thank my main mentor, Dr. Thomas Gutierrez, who helped assemble this whole report. With Dr. Gutierrez's aid, I was able to deliver an informative report on the field of gravitational wave detection that may someday prove to be useful to a rookie in the field.